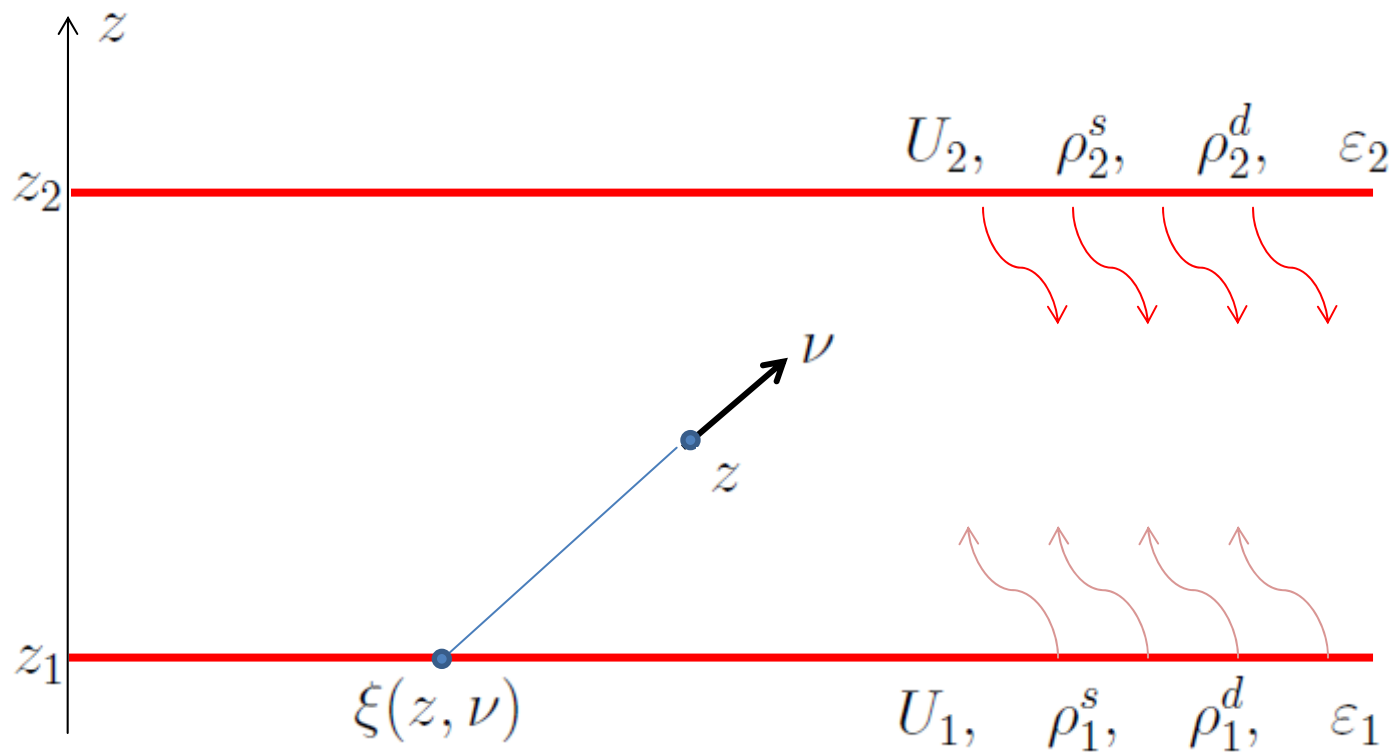


High-Performance Algorithm for the Coupled Conductive-Radiative Heat Transfer Problems

A.E. Kovtanyuk

Far Eastern National University, Vladivostok, Russia



$$X = (z_1, z_2) \times \{[-1, 0) \cup (0, 1]\}.$$

$$\Gamma^- = \{\{z_1 \times (0, 1]\} \cup \{z_2 \times [-1, 0)\}\}$$

Radiative heat transfer equation:

$$\nu f_z(z, \nu) + f(z, \nu) = c \int_{-1}^1 p(\nu, \nu') f(z, \nu') d\nu' + (1 - c)u^4(z), \quad (1)$$

$$f(z_i, \nu) = h(z_i) + (Bf)(z_i, \nu), \quad i = 1, 2, \quad (z_i, \nu) \quad (2)$$

$$h(z_i) = \varepsilon_i U_i^4, \quad (Bf)(z_i, \nu) = \rho_i^s f(0, -\nu) + 2\rho_i^d \int_0^1 f(0, -\text{sgn}(\nu)\nu) \nu d\nu.$$

Conductive heat transfer equation:

$$u''(z) = \frac{1}{2N_c} \left(\int_{-1}^1 f(z, \nu) \nu d\nu \right)' \quad (3)$$

$$u(0) = U_1, \quad u(d) = U_2. \quad (4)$$

Iterative procedure

$$\begin{aligned} \tilde{f}_0(z, \nu) = 0 &\longrightarrow u_0(z) = \frac{U_2 - U_1}{d}z + U_1 \xrightarrow{(1), (2)} \tilde{f}_1(z, \nu) \xrightarrow{(3), (4)} \\ \longrightarrow \tilde{u}_1(z) &\longrightarrow u_1(z) = \alpha \tilde{u}_1(z) + (1 - \alpha)u_0(z) \longrightarrow \dots \\ \longrightarrow \tilde{u}_k(z) &\longrightarrow u_k(z) = \alpha \tilde{u}_k(z) + (1 - \alpha)u_{k-1}(z) \end{aligned}$$

Consider the following expression

$$(Tf)(z, \nu) = (Bf)(\xi(\nu), \nu) \exp\left(-\frac{z - \xi(\nu)}{\nu}\right) + (ASf)(z, \nu),$$

here

$$(A\varphi)(z, \nu) = \frac{1}{\nu} \int_{\xi(\nu)}^z \exp\left(-\frac{z - z'}{\nu}\right) \varphi(z', \nu) dz',$$

$$(S\varphi)(z, \nu) = c \int_{-1}^1 p(\nu, \nu') \varphi(z, \nu') d\nu',$$

Solvability of the problem (1),(2)

Theorem 1. *Assuming that the inequalities $\|B\| \leq 1$ and $c < 1$ hold, there exists a unique solution of the problem (1),(2) that can be found in the form of the Neumann series*

$$f(z, \nu) = \sum_{k=0}^{\infty} (T^k f_0)(z, \nu) \quad (5)$$

converging in the norm of $C_b(X)$.

Recursive relations based on the Monte Carlo method:

$$u(z) = \frac{1}{2N_c} \int_0^z \int_{-1}^1 f(\zeta, \nu) d\zeta d\nu + C_1 z + C_2 \quad (10)$$

$$a(z) = \frac{1}{2N_c} \int_0^z \int_{-1}^1 f_N(\zeta, \nu) d\zeta d\nu \approx \frac{z}{MN_c} \sum_{k=1}^M \bar{f}_N(z_k, \nu_k),$$

Recursive algorithm based on the Monte Carlo method

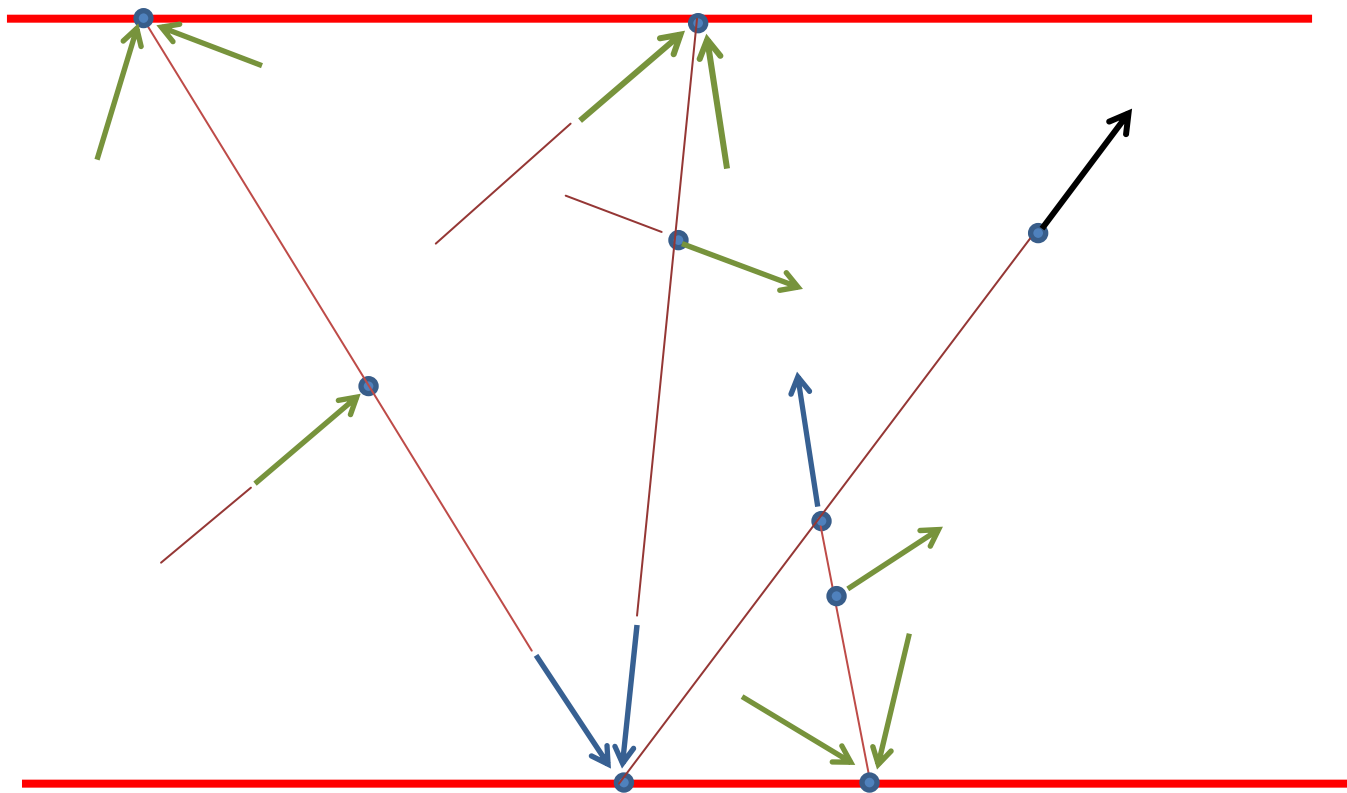
$$f_N(z, \nu) = \sum_{n=0}^N (T^n f_0)(z, \nu). \quad (7)$$

$$f_n(z, \nu) = (T f_{n-1})(z, \nu) + f_0(z, \nu), \quad n = 1, 2, \dots, N. \quad (8)$$

$$f_n(z, \nu) \approx \bar{f}_n(z, \nu) = \frac{1}{M} \sum_{k=1}^M s_k(z, \nu), \quad \bar{f}_0(z, \nu) = f_0(z, \nu), \quad (9)$$

$$s_k(z, \nu) = (B \bar{f}_{n-1})(\xi(\nu), \nu) \exp\left(-\frac{z - \xi(\nu)}{\nu}\right) + \\ + c \left(1 - \exp\left(-\frac{z - \xi(\nu)}{\nu}\right)\right) \bar{f}_{n-1}(z_k, \nu_k) + f_0(z, \nu).$$

Trajectory of the Monte Carlo method for $N = 2$



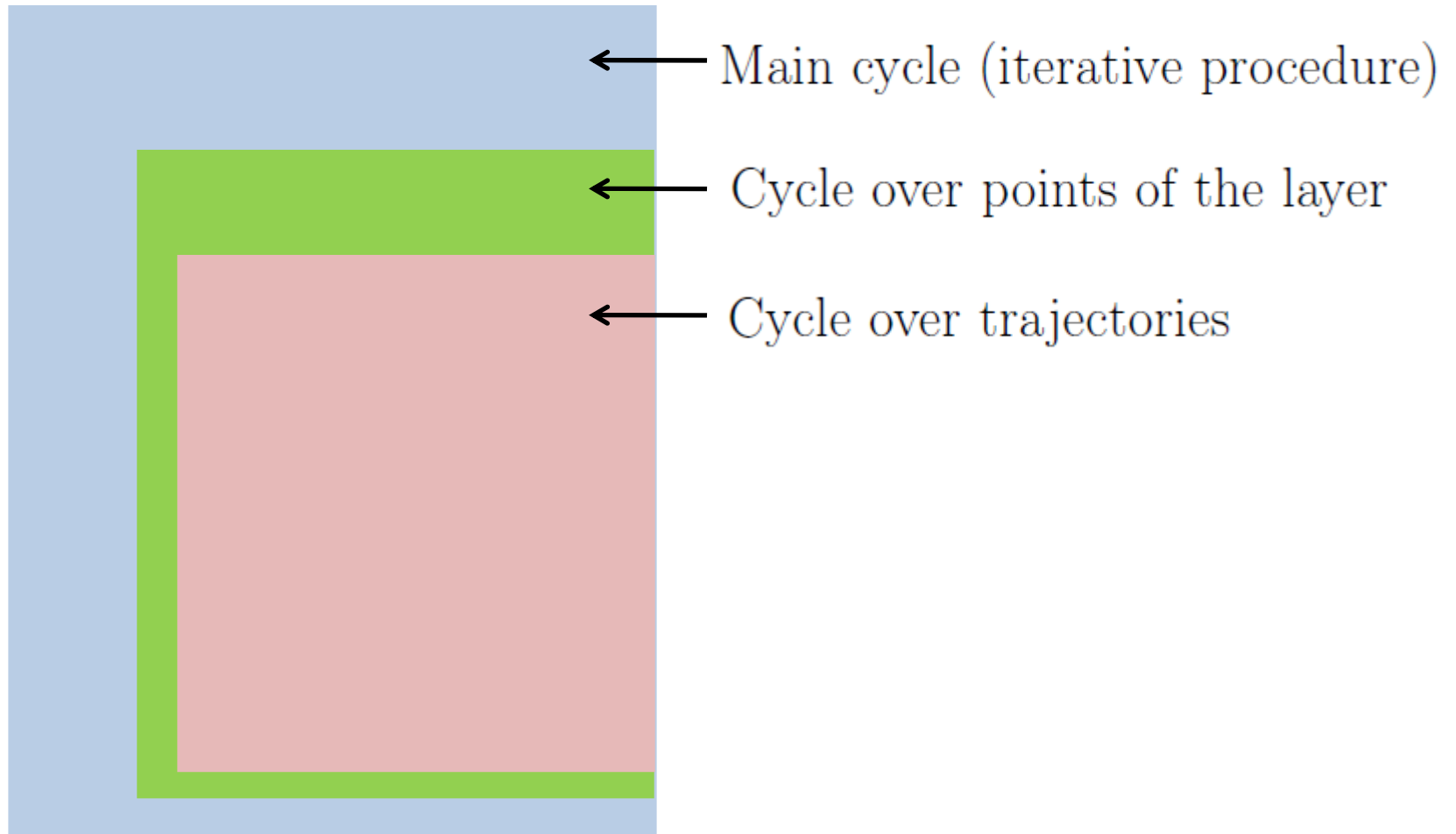
Complexity of the computing implementation:

1. An instability of the computing process. For more stability the generation of the large number of trajectories is needed. For computing of the solution in single point of the layer 10000 trajectories are used.
2. A slow convergence of the iterative procedure for case of the high temperature process (the case of small values N_c).
3. A number of the points in each trajectory increase as a sum of geometric series. For $N = 14$ the number of the points in single trajectory equals 7174452.

The ways of the parallelization of the computing process:

1. The calculation of the temperature at each point of the layer is performed by a separate thread.
2. The generation of each recursive trajectory of the Monte Carlo method is performed by a separate thread.

Structure of the program:



Diffusion approximation:

$$-\phi_0''(z) + 3(1 - c)\phi_0(z) = 3(1 - c)u^4(z), \quad (11)$$

$$\varepsilon_1\phi_0(0) - \frac{1}{2} \left(1 + \rho_1^s + \frac{4}{3}\rho_1^d \right) \phi_0'(0) = \varepsilon_1 U_1^4, \quad (12)$$

$$\varepsilon_2\phi_0(d) + \frac{1}{2} \left(1 + \rho_2^s + \frac{4}{3}\rho_2^d \right) \phi_0'(d) = \varepsilon_2 U_2^4. \quad (13)$$

$$u(z) = -\tilde{\sigma}\phi_0(z) + C_1z + C_2, \quad \tilde{\sigma} = \frac{1}{3N_c}. \quad (14)$$

Numerical experiments

$$c = 0.9, d = 3$$

$$U_1 = 1, \rho_1^s = 0.1, \rho_1^d = 0.2, \varepsilon_1 = 0.7$$

$$U_2 = 0.5, \rho_2^s = 0.3, \rho_2^d = 0.1, \varepsilon_2 = 0.6$$

$$N_c = 0.05; 0.00001$$

1. C.E. Siewert, J.R. Thomas, A computational method for solving a class of coupled conductive-radiative heat-transfer problems, J. Quant. Spectrosc. Radiat. Transfer, 45 (5) (1991) 273–281.
2. C.E. Siewert, An improved iterative method for solving a class of coupled conductive-radiative heat-transfer problems, J. Quant. Spectrosc. Radiat. Transfer, 54 (4) (1995) 599–605.

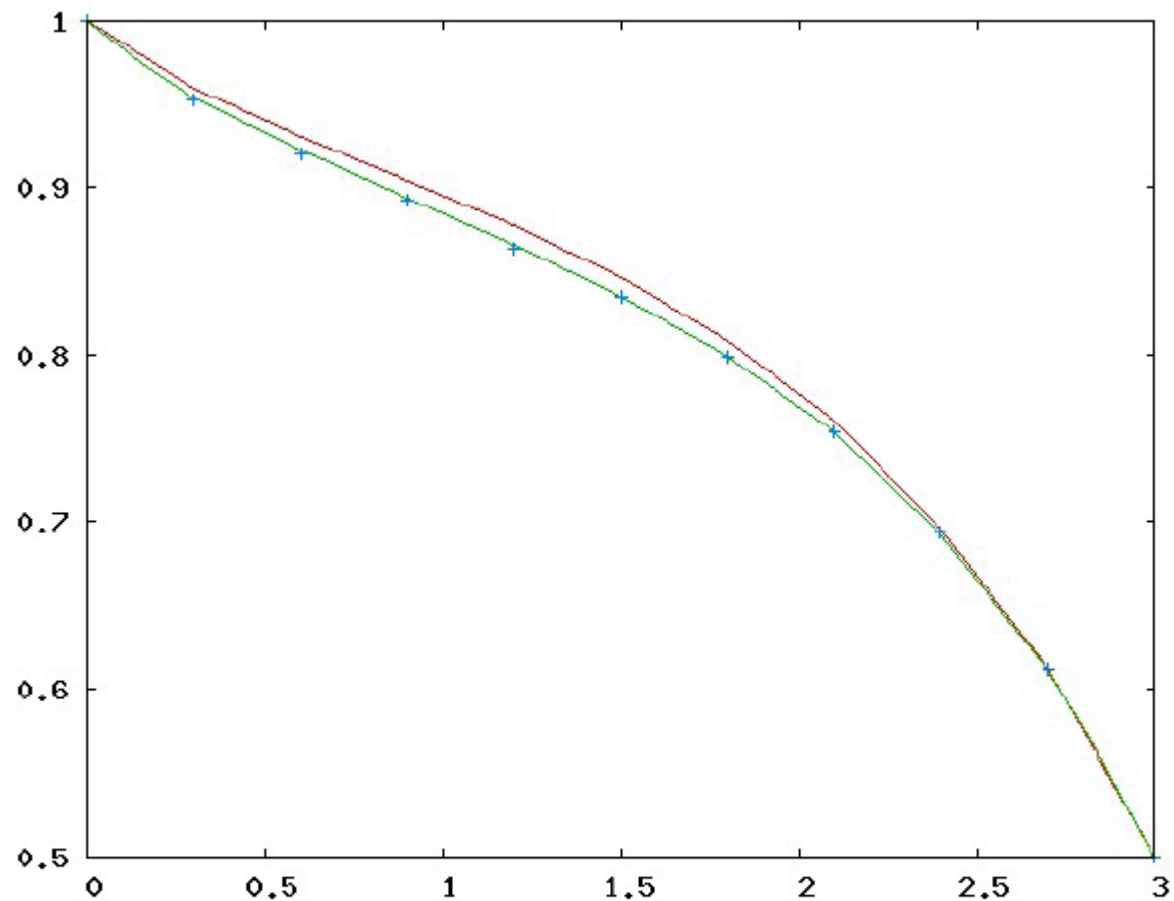


Fig. 1. The results of numerical simulation for $N_c = 0.05$ by the 20 steps of iterative algorithm based on: the Monte Carlo method, diffusion approximation in comparison with Siewert data (+)

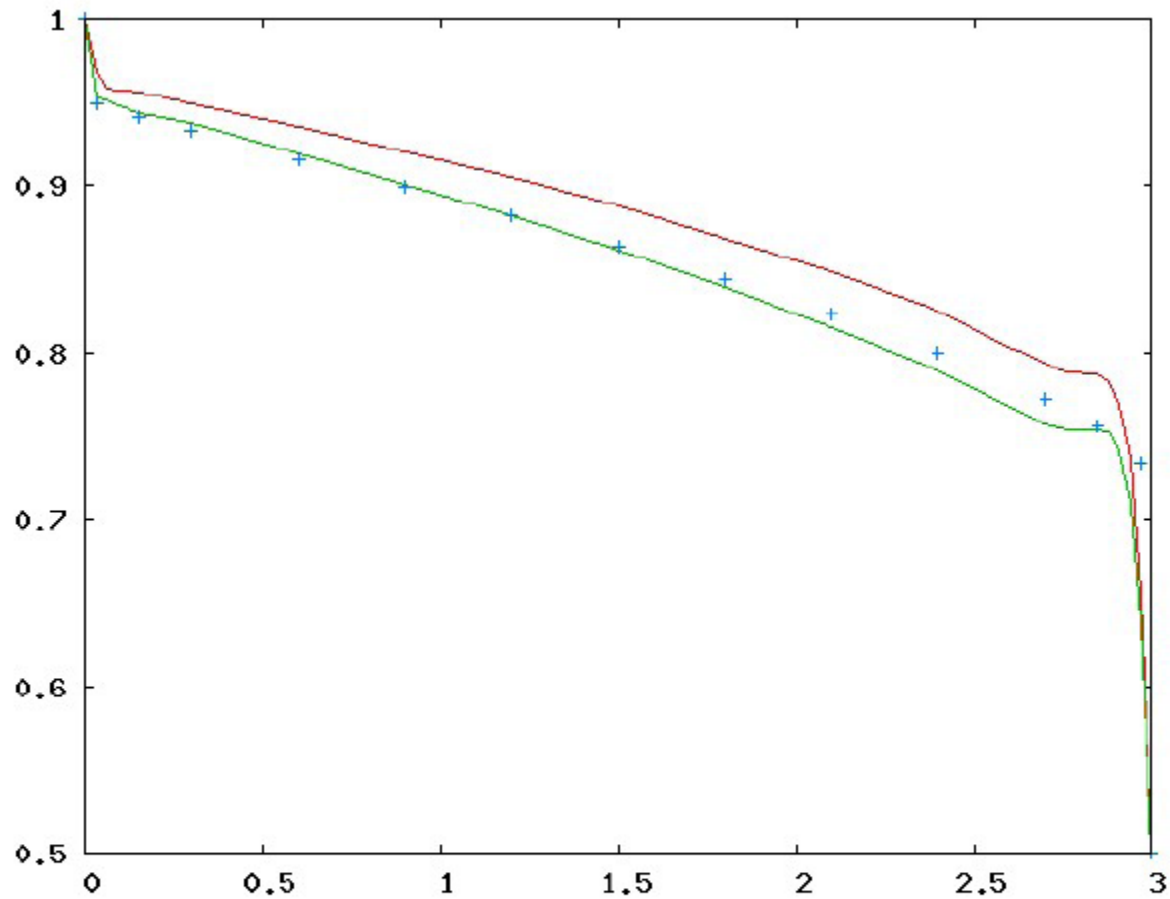


Fig. 2. The results of numerical simulation for $N_c = 0.00001$ by the 500 steps of iterative algorithm based on: the Monte Carlo method, diffusion approximation in comparison with Siewert data (+)

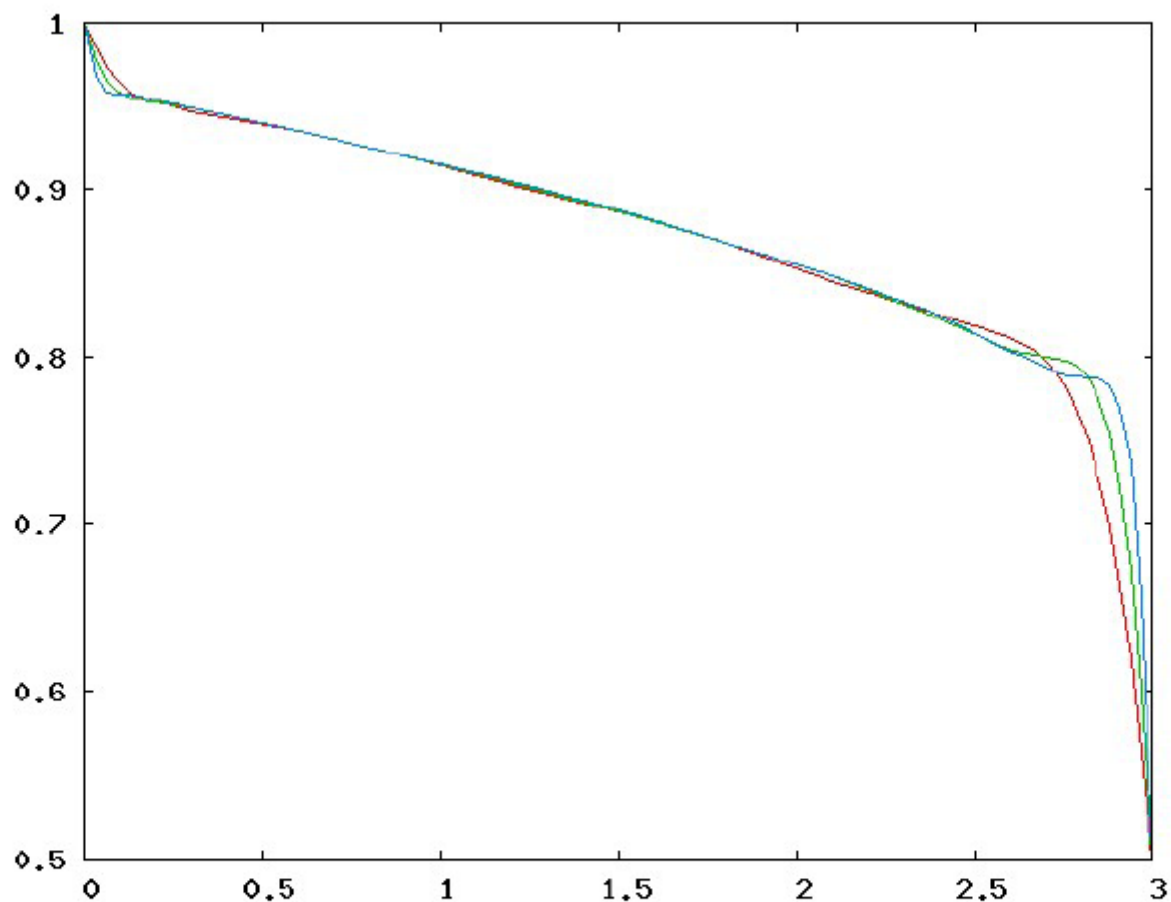


Fig. 3. The numerical experiments for $N_c = 0.00001$ which demonstrated a convergence of iterative procedure based on Monte Carlo method. The plots correspond to **50 steps** , **150 steps** and **500 steps** of the iterative procedure.

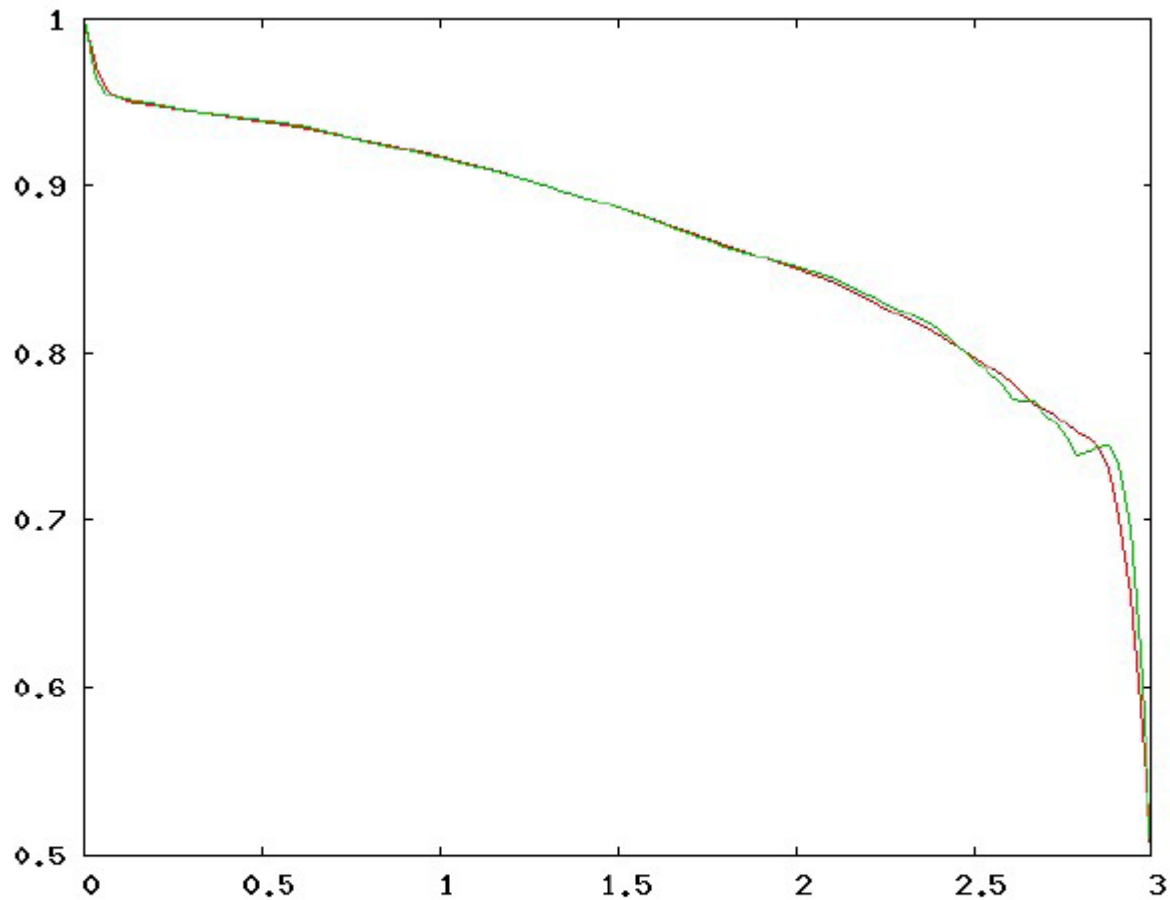


Fig. 4. The numerical experiments for $N_c = 0.00001$ which demonstrated instability of iterative procedure based on Monte Carlo method. This unsteadiness takes place for case insufficient number of trajectories. The plots correspond to **300 steps** and **900 steps** of the iterative procedure.


http://imcs.dvgu.ru/struc/kmf/dbase/ Google

Файл Правка Вид Избранное Сервис Справка

Google Поиск Дополнительно >> Войти

Избранное Database of radiological properties of materials, valua... Страница Безопасность Сервис

Database of radiological properties of materials valuable for x-ray diagnostics

 русский

[tables of poorly visible media](#) ■ [optimisation in tomography](#) ■ [directory of materials](#) ■ [references](#)

Authors

D.S. Anikonov¹, A.E. Kovtanyuk³, V.G. Nazarov², I.V. Prokhorov³,
N.S. Surovenko³, I.P. Yarovenko²

Introduction


Active work in determining radiological characteristics of different materials was started in the forties of the 20'th century, along with research dedicated to nuclear weapons and atomic energy. As of now large amount of experimental and theoretical data was obtained and is available in references and databases.

This database differs in that it's information is not about individual materials, but rather pairs of contacting materials. This organization scheme arose from the problem of determining a structure of heterogeneous media in x-ray tomography. In the industry this problem is related to non-damaging quality control of machine and machine parts, in medicine - analyzing damaged tissue, bones and organs.

D.S. Anikonov introduced a method for solving this problem, based on his notion of visibility measure [1] and integro-differential heterogeneity indicator [2]. Subsequent theoretical and numerical research is presented in works [3-33]. Among it are monographs [3-5] and Russian Federation patent [6] worth a special mention.

References

Database of radiological properties of materials valuable for x-ray diagnostics

 русский

[tables of poorly visible media](#) ■ [optimisation in tomography](#) ■ [directory of materials](#) ■ [references](#)

Tables of poorly visible media

Energy interval from MeV to MeV

Available materials


- HYDROGEN (1)
- HELIUM (2)
- LITHIUM (3)
- BERYLLIUM (4)
- BORON (5)
- SODIUM (11)
- MAGNESIUM (12)
- ALUMINUM (13)
- SILICON (14)
- PHOSPHORUS (15)
- SULFUR (16)
- CLORINE (17)
- ARGONE (18)
- POTASSIUM (19)
- CALSIUM (20)
- SCANDIUM (21)
- TITANIUM (22)
- VANADIUM (23)
- CROMIUM (24)
- MAMGANESE (25)



Selected materials

- CARBON. GRAPHITE (6)
- NITROGEN (7)
- OXYGEN (8)
- FLUORINE (9)
- NEON (10)

Database of radiological properties of materials valuable for x-ray diagnostics

 русский

[tables of poorly visible media](#) ■ [optimisation in tomography](#) ■ [directory of materials](#) ■ [references](#)

Optimisation in tomography


Material 1 (inclusion):

Distance to the inclusion (in cm):

Material 2 (medium):


Energy

from MeV to MeV

 [Instructions](#)



Database of radiological properties of materials valuable for x-ray diagnostics

 русский

[tables of poorly visible media](#) ■ [optimisation in tomography](#) ■ [directory of materials](#) ■ [references](#)


Chemical elements

- | | | | |
|----------------|------------------------|----------------|------------------|
| 1. Hydrogen | 6. Carbon,
graphite | 11. Sodium | 16. Sulfur |
| 2. Helium | 7. Nitrogen | 12. Magnesium | 17. Chlorine |
| 3. Lithium | 8. Oxygen | 13. Aluminum | 18. Argon |
| 4. Beryllium | 9. Fluorine | 14. Silicon | 19. Potassium |
| 5. Boron | 10. Neon | 15. Phosphorus | 20. Calcium |
| 21. Scandium | 26. Iron | 31. Gallium | 36. Krypton |
| 22. Titanium | 27. Cobalt | 32. Germanium | 37. Rubidium |
| 23. Vanadium | 28. Nickel | 33. Arsenic | 38. Strontium |
| 24. Chromium | 29. Copper | 34. Selenium | 39. Yttrium |
| 25. Manganese | 30. Zink | 35. Bromine | 40. Zirconium |
| 41. Niobium | 46. Palladium | 51. Antimony | 56. Barium |
| 42. Molybdenum | 47. Silver | 52. Tellurium | 57. Lanthanum |
| 43. Technetium | 48. Cadmium | 53. Iodine | 58. Cerium |
| 44. Ruthenium | 49. Indium | 54. Xenon | 59. Praseodymium |
| 45. Rhodium | 50. Tin | 55. Cesium | 60. Neodymium |
| 61. Promethium | 66. Dysprosium | 71. Lutetium | 76. Osmium |
| 62. Samarium | 67. Holmium | 72. Hafnium | 77. Iridium |
| 63. Europium | 68. Erbium | 73. Tantalum | 78. Platinum |
| 64. Gadolinium | 69. Thulium | 74. Tungsten | 79. Gold |

Интернет

100%

Database of radiological properties of materials valuable for x-ray diagnostics




 русский

[tables of poorly visible media](#) ■ [optimisation in tomography](#) ■ [directory of materials](#) ■ [references](#)

Tables of poorly visible media

Energy levels from 0.001 MeV to 20 MeV, where border between **SODIUM** and materials **NEON MAGNESIUM ALUMINUM SILICON** is poorly visible

Second medium	Energy (MeV)	Coefficients for: SODIUM				Coefficients for second medium			
		Absorbtion coefficient		Attenuation coefficient		Absorbtion coefficient		Attenuation coefficient	
12. MAGNESIUM	1.07210E-3	5.253E+2	6.137E+3	5.272E+2	6.248E+3	1.359E+3		1.363E+3	
12. MAGNESIUM	1.30500E-3	4.462E+3		4.536E+3		7.846E+2	9.239E+3	7.882E+2	9.473E+3
13. ALUMINUM	1.07210E-3	5.253E+2	6.137E+3	5.272E+2	6.248E+3	2.888E+3		2.894E+3	
13. ALUMINUM	1.55960E-3	2.869E+3		2.908E+3		9.716E+2	1.033E+4	9.773E+2	1.068E+4
14. SILICON	1.07210E-3	5.253E+2	6.137E+3	5.272E+2	6.248E+3	3.304E+3		3.311E+3	
14. SILICON	1.83890E-3	1.976E+3		2.000E+3		7.153E+2	7.127E+3	7.204E+2	7.437E+3

-  Coefficients jump for first medium
-  Coefficients jump for second medium
-  Coefficients jump for both media

Material 1 (inclusion):

Hydrogen

Distance to the inclusion (in cm):

1

Material 2 (medium):

Silicon

Energy

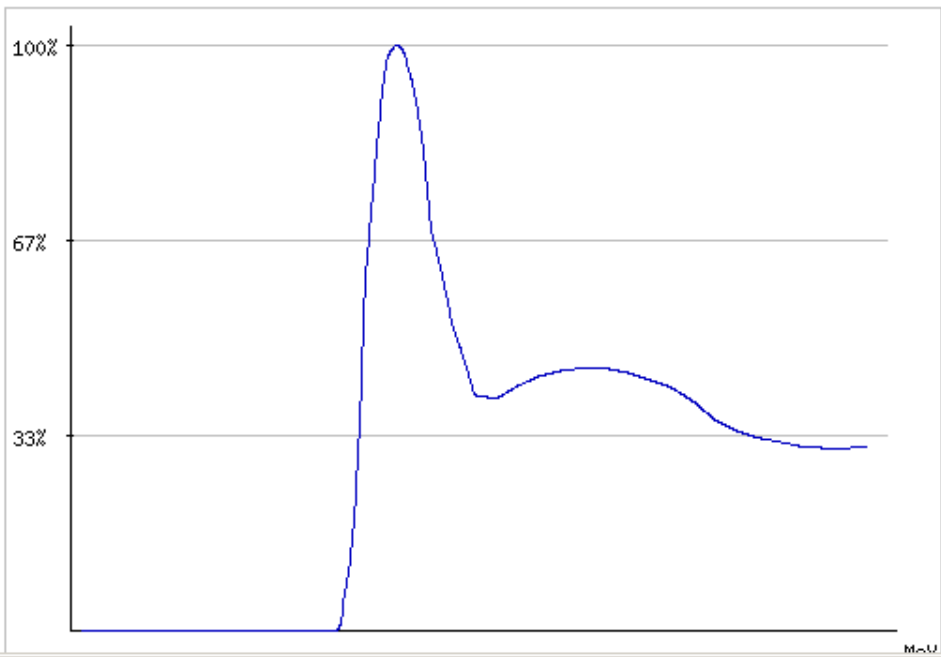
from 0.001 MeV to 20 MeV

Calculate

Instructions

Relative visibility of Hydrogen in the Silicon on the interval from 0.001 MeV to 20 MeV

Energy, MeV	Relative visibility, %
0.0010	0
0.0015	0
0.0018	0
0.0020	0
0.0030	0
0.0040	0
0.0050	0
0.0060	0
0.0080	0
0.0100	0
0.0150	0
0.0200	0
0.0300	5.48
0.0400	61.69



Thank you for attention!